ANALYTICAL AND NUMERICAL STUDIES OF LASER WAKEFIELD ACCELERATION IN BUBBLE REGIME

SONU KUMAR

DEPARTMENT OF PHYSICS

INDIAN INSTITUTE OF TECHNOLOGY DELHI

June 2023

ANALYTICAL AND NUMERICAL STUDIES OF LASER WAKEFIELD ACCELERATION IN BUBBLE REGIME

by

SONU KUMAR

Department of Physics

Submitted

in fulfillment of the requirements of the degree of Doctor of Philosophy

to the

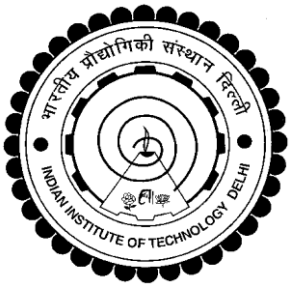

INDIAN INSTITUTE OF TECHNOLOGY DELHI

June 2023

Dedicated to

my family and loved ones

&

those

whoever inspired and encouraged me

Certificate

This is to certify that the thesis entitled "**Analytical and Numerical Studies of Laser Wakefield Acceleration in Bubble Regime**" being submitted by **Mr. Sonu Kumar** is worthy of consideration for the award of the degree of Doctor of Philosophy and is a record of the original bonafide research work carried out by him under our guidance and supervision, and that the results contained in it have not been submitted in part or full to any other university or institute for award of any degree / diploma.

We certify that he has pursued the prescribed course of research. We approve the thesis for the award of the degree of Doctor of Philosophy.

Hitendra K. Malik
Professor
Department of Physics
Indian Institute of Technology Delhi
INDIA

Dhananjay K. Singh
Assistant Professor
Department of Physics
P. K. Roy Memorial College
BBMK University Dhanbad
INDIA

Acknowledgements

First and foremost, I acknowledge my supervisor **Prof. Hitendra K. Malik** from IIT Delhi and co-supervisor **Dr. Dhananjay K. Singh** from PKRM College, Dhanbad for their constant support, guidance, and encouragement throughout the journey of Ph.D. In addition to around six years of research assistantship, they have supported me both academically and emotionally. They gave me the moral support during my most difficult times.

A sincere thanks to my SRC members: Prof. Amruta Mishra, Prof. R. K. Varshney and Prof. Ramesh Narayanan for their supportive remarks. I am grateful to my previous mentors Prof. Bipul Kumar Sinha, Prof. Rakesh Singh Moirangthem, Prof. Binata Panda, and Prof. Shougajim Somorendro Singh for their ongoing encouragement.

Dr. Rajat Dhawan, Chandan Vishwakarma, Amal Jahan, and other friends deserve my gratitude for their invaluable feedback and encouragement throughout my doctoral studies. My fellow labmates Dr. Dimple Tuteja, Dr. Rashmi Shrivastava, Dr. Sheetal Punia, Sandeep, Dhananjay Verma, Rakesh Kumar, Mohit Kumar and Subhajit Bhasker deserve special recognition for *the fun times we had working and socializing together*.

I am grateful to my siblings: Mr. Sachit K. Gupta and Mrs. Sushma Kumari and my parents: Sh. Rajendra Prasad and Smt. Laxmi Devi who are remembering me in their prayers for the ultimate success. Without them, I consider myself nothing. I could accomplish any goal only because of their motivation, encouragement, and moral support.

I acknowledge Department of Physics, Indian Institute of Technology Delhi for the financial support throughout this study. I acknowledge developers of SMILEI codes and high-performance computing (HPC) clusters at Indian Institute of Technology Delhi for providing the requested diagnostics and facilitating Particle-In-Cell simulations.

At last, but not the least, I acknowledge most – powerful, Almighty God for each and everything.

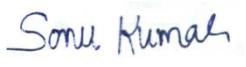

(Sonu Kumar)

Abstract

Plasma wakefield acceleration is a promising technique to build compact and powerful particle accelerators. In such accelerators, the electric fields required to accelerate charged particles are sustained by electron density modulations in the plasma which may be excited by a short intense laser pulse propagating through the plasma. The radiation pressure of the laser pushes away the plasma electrons which are pulled back by ions which are considered to be stationary due to their heavier mass. This initiates a charge density oscillation behind the laser pulse referred to as plasma wakefield, similar to the wake of a boat in a river. A bunch of electrons injected into this wakefield are constantly pulled towards the pulse and get accelerated to a good fraction of the speed of light very quickly. This scheme of particle acceleration is known as Laser-Plasma Wakefield Acceleration (LWFA). An ultra-intense ($> 10^{18}\, W/cm^2$) laser pulse having a pulse length shorter than the plasma wavelength expels the electrons from a region due to the trapping of electromagnetic energy and creates ion cavities or bubbles. The expelled plasma electrons are accumulated around the bubble surface and some of them are self-injected into the wakefield and get accelerated. The bubble regime of electron acceleration has the advantage that no external electron injection mechanism is needed as the electrons are self-injected and also no preformed plasma channel is required for the electron acceleration since the bubbles can guide the laser pulse up to many Rayleigh lengths.

This thesis describes both analytical and numerical studies for LWFA in the bubble regime. Various shapes of bubbles such as spherical, longitudinal-ellipsoid or transverse-ellipsoid are found to be controlled by d'Alembert equations under three different Gauge conditions. For each of the Gauge conditions, wakefield potential inside various shapes of the bubbles has been calculated analytically and is applied to numerically investigate the self-injection of plasma electrons in the bubble. Several parameters such as bubble velocity, bubble radius and impact parameters are described and their effect on bubble formation and self-injection of electrons have been studied numerically solving the coupled differential equations. Particle-In-Cell (PIC) simulations have been performed to numerical model the experimental conditions for LWFA to understand various complex kinetic and relativistic phenomena of laser-plasma interactions which have not been addressed experimentally. The simulations have been performed using the PIC code *Smilei* which is a high-performance open-source code for the simulation of relativistic laser-plasma interaction. The focus of these simulations lies in the optimization of laser pulse specifications and plasma density profiles for efficient particle acceleration in the bubble regime of LWFA. In this regard, the study of wakefield generation by the modulation of various plasma density profiles has been presented. To benchmark the

experimental conditions, a comparison has been presented for various temporal and spatial profiles of laser vis-à-vis the plasma density modulation, wakefield strength, electrons self-injection, energy spectrum and kinetic energy gradient of accelerated electrons. The scheme of multi-pulse laser wakefield acceleration (MP-LWFA) has been investigated and the merits of the multi-pulse LWFA over single-pulse LWFA has been demonstrated. The work described in this thesis attempts to benchmark the experimental conditions required to explore various aspects of laser plasma wakefield acceleration.

सार

प्लाज्मा वेकफील्ड त्वरण कॉम्पैक्ट और शक्तिशाली कण त्वरक बनाने के लिए एक आशाजनक तकनीक है। ऐसे त्वरक में, आवेशित कणों को गति देने के लिए आवश्यक विद्युत क्षेत्र प्लाज्मा में इलेक्ट्रॉन संख्या घनत्व मॉडुलेशन द्वारा बनाए रखा जाता है जो प्लाज्मा के माध्यम से फैलने वाली एक छोटी तीव्र लेजर पल्स द्वारा उत्तेजित हो सकता है। लेजर का विकिरण दबाव प्लाज्मा इलेक्ट्रॉनों को दूर धकेलता है जो आयनों द्वारा वापस खींच लिए जाते हैं जिन्हें उनके भारी द्रव्यमान के कारण स्थिर माना जाता है। यह प्लाज्मा वेकफील्ड के रूप में संदर्भित लेजर पल्स के पीछे एक चार्ज घनत्व दोलन शुरू करता है, जो नदी में नाव के चलने के समान होता है। इस वेकफील्ड में प्रेषित किए गए इलेक्ट्रॉनों का एक गुच्छा लगातार पल्स की ओर खींचा जाता है और बहुत तेज़ी से प्रकाश की गति के एक अच्छे अंश तक त्वरित हो जाता है। कण त्वरण की इस योजना को लेजर-प्लाज्मा वेकफील्ड त्वरण के रूप में जाना जाता है। एक अति तीव्र $\left(>10^{18}\text{वॉट/सेमी}^2\right)$ लेज़र पल्स, जिसकी स्पंद लंबाई प्लाज्मा तरंग दैर्ध्य से कम होती है, विद्युत चुम्बकीय ऊर्जा के फंसने के कारण एक क्षेत्र से इलेक्ट्रॉनों को बाहर निकाल देता है और आयन गुहा या बबल बनाता है। निष्कासित प्लाज्मा इलेक्ट्रॉन बबल की सतह के चारों ओर जमा होते हैं और उनमें से कुछ को वेकफील्ड में स्व-प्रेषित किया जाता है और त्वरित हो जाता है। इलेक्ट्रॉन त्वरण के बबल व्यवस्था का लाभ यह है कि किसी बाहरी इलेक्ट्रॉन प्रेषण तंत्र की आवश्यकता नहीं होती है क्योंकि इलेक्ट्रॉन स्वयं प्रेषित होते हैं और इलेक्ट्रॉन त्वरण के लिए किसी पूर्वनिर्मित प्लाज्मा चैनल की भी आवश्यकता नहीं होती है क्योंकि बबल लेजर पल्स को कई रैले लंबाई तक निर्देशित कर सकते हैं।

यह शोध-ग्रंथ बबल क्षेत्र में लेजर वेकफील्ड त्वरण के लिए विश्लेषणात्मक और संख्यात्मक दोनों अध्ययनों का वर्णन करती है। बबल के विभिन्न आकार जैसे गोलाकार, अनुदैर्ध्य-दीर्घवृत्ताभ या अनुप्रस्थ-दीर्घवृत्ताभ तीन अलग-अलग गेज स्थितियों के तहत डी'अलेम्बर्ट समीकरणों द्वारा नियंत्रित पाए जाते हैं। गेज स्थितियों में से प्रत्येक के लिए, बबल के विभिन्न आकारों के अंदर वेकफील्ड क्षमता की गणना विश्लेषणात्मक रूप से की गई है और इसे बबल में प्लाज्मा इलेक्ट्रॉनों के स्व-प्रेषण की संख्यात्मक रूप से जांच करने के लिए लागू किया गया है। बबल वेग, बबल त्रिज्या और प्रभाव मापदंडों जैसे कई मापदंडों का वर्णन किया गया है और बबल गठन और इलेक्ट्रॉनों के स्व-प्रेषण पर उनके प्रभाव का संख्यात्मक रूप से युग्मित अंतर समीकरणों को हल करने का अध्ययन किया गया है। पार्टिकल-इन-सेल (पीआईसी) सिमुलेशन लेजर-प्लाज्मा इंटरैक्शन के विभिन्न जटिल गतिज और सापेक्ष घटनाओं को समझने के लिए लेजर वेकफील्ड त्वरण के लिए प्रायोगिक स्थितियों के संख्यात्मक मॉडल के लिए किए गए हैं जिन्हें प्रयोगात्मक रूप से संबोधित नहीं किया गया है। पीआईसी कोड स्माइली का उपयोग करके

सिमुलेशन का प्रदर्शन किया गया है जो सापेक्षवादी लेजर-प्लाज्मा मिलाप के सिमुलेशन के लिए एक उच्च-प्रदर्शन खुला-स्त्रोत कोड है। इन सिमुलेशन का ध्यान लेजर वेकफील्ड त्वरण के बबल क्षेत्र में कुशल कण त्वरण के लिए लेजर पल्स विनिर्देशों और प्लाज्मा घनत्व प्रोफाइल के अनुकूलन में निहित है। इस संबंध में, विभिन्न प्लाज्मा घनत्व प्रोफाइल के मॉडुलेशन द्वारा वेकफील्ड उन्मूलन का अध्ययन प्रस्तुत किया गया है। प्रयोगात्मक स्थितियों को बेंचमार्क करने के लिए, प्लाज्मा घनत्व मॉडुलेशन, वेकफील्ड परिमान, इलेक्ट्रॉन स्व-प्रेषण, ऊर्जा वर्णक्रम और त्वरित इलेक्ट्रॉनों की गतिज ऊर्जा प्रवणता की तुलना में लेजर के विभिन्न लौकिक और स्थानिक प्रोफाइल के लिए एक तुलना प्रस्तुत की गई है। बहू -पल्स लेजर वेकफील्ड त्वरण की योजना की जांच की गई है और एक -पल्स लेजर वेकफील्ड त्वरण पर बहू -पल्स लेजर वेकफील्ड त्वरण की खूबियों का प्रदर्शन किया गया है। इस शोध-ग्रंथ में वर्णित कार्य लेजर प्लाज्मा वेकफील्ड त्वरण के विभिन्न पहलुओं का पता लगाने के लिए आवश्यक प्रायोगिक स्थितियों को बेंचमार्क करने का प्रयास किया गया है।

Table of Contents

List of Figures

Figure 2.8: Variation of maximum energy gain W_{max} along y-direction with relativistic Lorentz factor γ_p along x-direction with the change of transverse geometrical coefficient C.

Figure 2.9: Variation of wakefield potential $\Phi = \left(\frac{1}{4} - \mathrm{C}\right)\zeta^2 + \frac{y^2}{4}$ along (ζ, y) direction with changing of transverse coefficient C.

Figure 2.10: Variation of accelerating field or wakefield E_x along y – direction with bubble radius r_b along propagation direction x- axis with the change of transverse geometrical coefficient C.

Figure 2.11: Variation of maximum energy gain W_{max} along y-direction with relativistic Lorentz factor γ_p along x-direction with the change of transverse geometrical coefficient C.

Figure 3.1: This figure shows the parameters related with bubble and $R = \sqrt{{\zeta_0}^2 + \rho^2}$ is bubble radius, where ζ_0 and $y_0 = \rho$ are longitudinal and transverse coordinates.

Figure 3.2: Trajectory of electrons with variation of shapes of the bubble with C = 0 (spherical bubble), C= – 0.2 (transverse ellipsoid bubble) and C= 0.2 (longitudinal ellipsoid bubble) when $p_{x0} = 0, p_{y0} = 0, \zeta_0 = \sqrt{R^2 - y_0^2}, y_0 = \rho = 10$ and bubble velocity $\mathrm{V} = 0.969$ for Lorentz factor $\gamma_0 = 4$. Here radius of the bubble $\mathrm{R} = 10$.

Figure 3.3: Longitudinal phase-space diagram of trapped electrons in different shaped bubble with C = 0 for spherical bubble (a), with C = 0.2 for longitudinal ellipsoid bubble (b) and with C = -– 0.2 for transverse ellipsoid bubble (c), when V = 0.969 for $\gamma_0 = 4$ with impact parameter of the trapped electron as $\rho = 10$ and radius of the bubble as R = 10.

Figure 3.4: Transverse phase-space diagram of the trapped electrons in different shaped bubble when C = 0 (spherical bubble) in (a), C = 0.2 (longitudinal ellipsoid bubble) in (b) and C = – 0.2 (transverse ellipsoid bubble) in (c) V = 0.969 for $\gamma_0 = 4$ with impact parameter of the trapped electron as $\rho = 10$ and radius of the bubble as R = 10.

Figure 3.5: Trajectory of the electrons in spherical bubble at C = 0 and with initial electrons momentum value $p_{x0} = 0, p_{y0} = 0, \zeta_0 = \sqrt{R^2 - y_0^2}$, and $\mathrm{V} = 0.969$ for Lorentz factor $\gamma_0 = 4$. Here radius of the bubble is $\mathrm{R} = 10$ with different values of impact parameter $y_0 = \rho$.

Figure 3.6: Trajectory of the electrons in longitudinal ellipsoid bubble at C = 0.2 and with initial electrons momentum value $p_{x0} = 0, p_{y0} = 0, \zeta_0 = \sqrt{R^2 - y_0^2}$, and $\mathrm{V} = 0.969$ for Lorentz factor $\gamma_0 = 4$. Here radius of the bubble is $\mathrm{R} = 10$ with different values of impact parameter $y_0 = \rho$.

Figure 3.7: Trajectory of the electrons in transverse ellipsoid bubble at C = 0.2 and with initial electrons momentum value $p_{x0} = 0, p_{y0} = 0, \zeta_0 = \sqrt{R^2 - y_0^2}$, and $\mathrm{V} = 0.969$ for Lorentz factor $\gamma_0 = 4$. Here radius of the bubble is $\mathrm{R} = 10$ with different values of impact parameter $y_0 = \rho$.

Figure 3.8: Trajectory of the electrons in spherical bubble at C = 0.0 and with bubble velocity V = 0.969 for Lorentz factor $\gamma_0 = 4$. Here the impact parameter is $\rho = 6$ with different values of bubble radius $R_1 = 10, R_2 = 8, R_3 = 6$.

Figure 3.9: Trajectory of the electrons in longitudinal ellipsoid bubble at C = 0.2 and with bubble velocity V = 0.969 for Lorentz factor $\gamma_0 = 4$. Here the impact parameter is $\rho = 6$ with $R_1 = 10, R_2 = 8, R_3 = 6$.

Figure 3.10: Trajectory of the electrons in transverse ellipsoid bubble at C = – 0.2 and with bubble velocity V = 0.969 for Lorentz factor $\gamma_0 = 4$. Here the impact parameter is $\rho = 6$ with $R_1 = 10, R_2 = 8, R_3 = 6$.

Figure 3.11: Trajectory of the electrons in spherical bubble at $C = 0.0$ with bubble radius $R = 10$ and impact parameter $\rho = 10$. Here, different bubble velocities have been considered as $V_1 = 0.980, V_{2=}0.969, V_3 = 0.944$.

Figure 3.12: Trajectory of the electrons in longitudinal ellipsoid bubble at $C = 0.2$ with bubble radius $R = 10$ and with impact parameter $\rho = 10$. Here, different bubble velocities have been considered as $V_1 = 0.980, V_{2=}0.969, V_3 = 0.944$.

Figure 3.13: Trajectory of the electrons in transverse ellipsoid bubble at $C = -0.2$ with bubble radius $R = 10$ and impact parameter $\rho = 10$. Here, different bubble velocities have been considered as $V_1 = 0.980, V_{2=}0.969, V_3 = 0.944$.

Figure 4.1: Laser field E_y transverse to the propagation direction. Fig.4.1(a) represents the laser field for Gaussian laser pulse and fig.4.1 (b) represents the laser field for trapezoidal laser pulse at $t = 100\ fs$.

Figure 4.2: Longitudinal electric field i.e. accelerating field $E_x\ (TV/m)$ along the direction of beam propagation at time $t = 2.4\ ps$. The solid line represents the electric field for a temporal Gaussian laser pulse and the dashed line represents the electric field for a temporal trapezoidal pulse.

Figure 4.3: Variation of longitudinal electric field $E_x\ (TV/m)$ along (x, y) grid at time $t = 2.4\ ps$ for temporal Gaussian laser pulse profile (a) and for temporal trapezoidal laser pulse profile (b).

Figure 4.4: Plasma electrons density for temporal Gaussian laser pulse driven LWFA in 4.4(a, c, e) and for temporal trapezoidal laser pulse driven LWFA in 4.4(b, d, f) at simulation time $t = 1.3\ ps, 2.0\ ps, 2.4\ ps$.

Figure 4.5: Comparison of accelerated electrons kinetic energy spectra for Gaussian laser pulse (a) for trapezoidal laser pulse (b) at $t = 2.4\ ps$.

Figure 4.6: Line spectra of accelerated electrons with their kinetic energy along x axis and corresponding electron number/GeV along y axis at time $t = 2.4\ ps$. Solid line represents line spectra for Gaussian pulse and dashed line represents line spectra for trapezoidal pulse.

List of Symbols

a_0 : Laser strength parameter

A : Normalized vector potential

A_x : Normalized vector potential along x-axis

A_y : Normalized vector potential along y-axis

A_z : Normalized vector potential along z-axis

$A_\perp$: Normalized transverse vector potential

a : Longitudinal geometrical coefficient associated with wakefield potential

b : Transverse geometrical coefficient associated with wakefield potential

B : Magnetic field (magnitude)

B_x : Magnetic field along x-axis

B_y : Magnetic field along y-axis

B_z : Magnetic field along z-axis

c : Speed of light in free space

C or C : Geometrical coefficient associated with transverse vector potential

$\mathrm{C}_1, \mathrm{C}_2, \mathrm{C}_3, \mathrm{C}_4, \mathrm{C}_5$: Different sets of Geometrical coefficient associated with transverse vector potential

E : Electric field (magnitude)

E_0 : Maximum electric field (magnitude)

E_x : Electric field along x-axis

E_y : Electric field along y-axis

E_z : Electric field along z-axis

E_{pulse} : Energy of the laser pulse

$-e$: Charge of an electron

ε_0 : Electrical permittivity in free space

η : Geometrical parameter

F : Restoring force according to Hooke's law

F_e : Lorentz force

f : Distribution function

H : Hamiltonian equation

I : Intensity of laser

I_0 : Maximum intensity of laser

I_{18} : Intensity in the units of $10^{18}\ W/cm^2$

J : Current density (magnitude)

J_x : Current density along x-axis

$J_\perp$: Transverse current density

k : Spring constant

k_p : Plasma wavevector

K : Transverse geometrical coefficient

L_d : Dephasing length

λ or λ_0 : Laser's wavelength

λ_p : Plasma wavelength

$\lambda_{\mu m}$: Laser's wavelength in micrometer

m_e : Mass of an electron

n : number of laser pulse

n_e : Initial plasma electron density

n_a : Residual electron density

n_0 : Ambient plasma electron density

n_c : Critical density of plasma electrons

p : Momentum of electron (magnitude)

p_x : Longitudinal kinetic momentum of electrons

p_{x0} : Initial kinetic momentum of electrons along x-axis

p_x : Longitudinal kinetic momentum of electrons

p_{y0} : Initial kinetic momentum of electrons along y-axis

p_y : Transverse kinetic momentum of electrons

P_x : Longitudinal canonical momentum of electrons

P_y : Transverse canonical momentum of electrons

P_{peak} : Peak power of laser system

P_c : Threshold power of laser system

ϕ : Scalar potential

Φ or Ψ : Wakefield potential

r : Three-dimensional position

r_b or R or R_b: Radius of the bubble

R_1, R_2, R_3 : Different sets of the radius of the bubble

r_0 : Plasma length

ρ_e : Charge density of electron

ρ : Impact parameter

ρ_1, ρ_2, ρ_3 : Different sets of impact parameter

t : Actual time

t_1 : Time at first position

t_2 : Time at second position

τ_G : Time at HWHM

τ_L : Laser's period

τ_p : Time at FWHM

v : Velocity of electrons

v_x : Velocity of electrons along x-axis

v_g : Group velocity of the laser pulse

v_{etch} : Etching velocity of the photons

v_{ph} : Phase velocity of the wakefield

v_b or V : Bubble velocity

V_1, V_2, V_3 : Different sets of bubble velocity

w_G : Spot size at HWHM

w_0 : Spot size at FWHM

ω_p: Plasma frequency

ω or ω_0 or ω_L: Laser's frequency

W_{max} or W_{gain} : Energy gain

x : Position along x-axis

x_1 : Position along x-axis in first position

x_2 : Position along x-axis in second position

γ : Lorentz factor

γ_p : Lorentz factor w.r.t. bubble velocity

γ_0 : Initial Lorentz factor w.r.t. bubble velocity

y : Position along y-axis

y_0 : Initial position of impact parameter

ξ or ζ : Normalized distance

ζ_0 : Initial normalized distance

z : Position along z-axis

List of Tables